JOURNAL OF MATERIALS SCIENCE 30 (1995) 1811–1817

Kinetics of WC–Co oxidation accompanied by swelling

F. LOFAJ
Institute of Materials Research SAS, Watsonova 47, 043 53 Košice, Slovakia
YU. S. KAGANOVSKII
Kharkov State University, Dept. of Crystal Physics, Freedom Sq. 3, 310 077 Kharkov, Ukraine

The oxidation behaviour of WC–Co sintered carbides with 3–5 μm grain size of WC and 6–15 vol.% of cobalt have been studied in air in the temperature range 650–800 °C. The intensive swelling of up to 350% of initial specimen size and linear kinetics of the growth of the porous WO_3 layer were observed during the oxidation. The final shape of the specimen after oxidation was dependent on its initial shape. The apparent activation energy of the dimension and weight gain kinetics were within the range 32–67 kJ mol^{-1} and the process was proposed to be controlled by the reaction at the interface. The oxidation rates and swelling coefficients increased when the mean size of WC grains was decreased and cobalt content increased. The possible model of WC–Co alloys' oxidation and swelling was proposed for the observed shape development and kinetics of oxidation.

1. Introduction

Tungsten carbide alloys are well-known engineering materials widely used for cutting tools because of their high hardness, strength and wear resistance [1–3]. However, the application of hard metals at high temperatures can be limited by their oxidation – even relatively short-time surface oxidation can cause significant reduction of the strength of WC–Co [4].

The parabolic like weight gain kinetics and the formation of brittle oxide layers have been reported after the oxidation of WC and WC–Co systems in the temperature range 600–1000 °C [5–8]. The addition of 6% of Co slightly decreased the oxidation rate in comparison with pure WC [5]. Similar behaviour was observed during the oxidation of WC–Ni–Al alloys [9].

Detailed studies [9–11] revealed the dependence of oxidation rate of sintered carbides on the oxygen partial pressure. However, the mechanisms of the oxidation were not described in these works. The investigation of the oxidation behaviour of a similar system, TiC powders, showed several fast and slow stages and different activation energies at different temperatures [11]. The variety of factors influencing the oxidation of sintered carbides requires more detailed study of its kinetics over the wide temperature range.

The aim of the present work was to study the kinetics and mechanism of oxidation of sintered WC–Co alloys with different microstructures.

2. Material characterization and experimental methods

The oxidation experiments were carried out on 4 grades of WC–Co alloys produced in Pramet Šumperk (Czech Republic) containing 6, 10 and 15 vol.% of Co and with 3 and 5 μm mean size of WC grains. The porosity of all samples was less than 1%. The specimens had the shape of cylinders (diameter 7 mm, height 13 mm) or cubes (side 5 mm) with polished surfaces.

The isothermal annealing of specimens in air was performed under atmospheric pressure at 650, 700, 750 and 800 °C, respectively. Vertical elongation within the range of 2 mm was measured continuously by inductive transducer. When the dimensional change exceeded the transducer range heat treatment was periodically interrupted, samples were rapidly cooled and weight gain and dimensional changes (length and diameter in the case of cylinders and all sides in cubic specimens) were measured at room temperature. The microstructure of as-received and oxidized samples were observed by optical and scanning electron microcopy (SEM). The phases present in the sample after the oxidation were identified by X-ray diffraction (CuK_α) and by electron microdiffraction in a transmission electron microscope under an accelerating voltage of 90 kV on fine oxide particles which were dispersed in carbon replicas.

3. Results

The extensive brittle porous oxide layer formation was observed on all samples over the whole studied temperature range. Monoclinic WO_3 phase in oxidized layers and a small amount of Co, CoO and unoxidized WC were identified by X-ray diffraction. The electron microdiffraction in TEM confirmed the presence of WO_3. Time dependence of weight gain showed

0022–2461

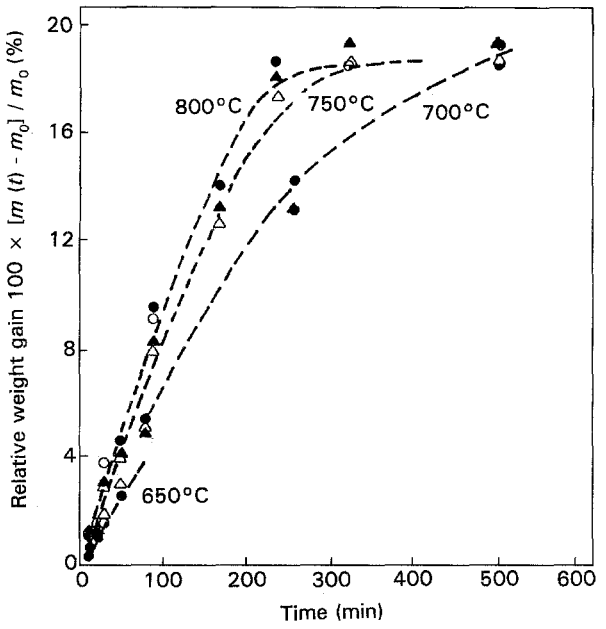

Figure 1 Relative weight gain kinetics of WC–Co alloys with different grain size and Co content after oxidation at different temperatures. ○, 6% Co/3 μm WC; △, 6% Co/5 μm WC; ▲, 10% Co/5 μm WC; ●, 15% Co/3 μm WC.

non-linear, parabolic-like behaviour (Fig. 1) and the maximum relative weight gains after the complete oxidation reached approximately 18.5–19% depending on the content of Co and mean size of WC grains.

The shape of specimens changed considerably during the oxidation: cylindrical specimens were transformed to "rotors" with several radial "blades" and two cones on the axis (Fig. 2), while the cubic specimens – to a 3-dimensional cross (Fig. 3). The difference between oxidized cylindrical and cubic specimens consisted also in the formation of regular pyramids without cracks from the flat sides of a cube instead of cones, which grew from the base planes of a cylinder. The successive shape development of a cylindrical specimen from Fig. 2a–c can be seen in the scheme in Fig. 4. The angles at the top of the cone 2β at different temperatures and for the specimens with various microstructure parameters are summarized in Table I.

In contrast to weight gain behaviour, both continuous and interrupted dilatometric measurements of the vertical elongation of samples showed approximately linear kinetics (Fig. 5). The maximum relative elongation $\Delta H(t_{max})/H_0$, (where $\Delta H = H(t) - H_0$ (H_0, initial specimen height (length); $H(t)$, time dependence of the height of specimen; t time of oxidation; t_{max}, time to complete oxidation)) reached almost 350% (see Fig. 5).

The SEM observation of the cross-sections (perpendicular to the cylinder axis) of partially oxidized specimens revealed a very porous microstructure of oxidation products (Fig. 6a) and a sharp boundary between the oxide layer and unoxidized WC–Co (indicated by arrow on Fig. 6b). The linear dimensions (radius and height) of the unoxidized part of the cylindrical samples decreased linearly with the same rate in both radial and longitudinal directions (Fig. 7). The thickness of the oxide layer also increased linearly with time (Fig. 7). When it attained approximately 0.1 mm, large radial cracks appeared and separated the layer into several parts. These isolated parts of the oxide layer grew linearly with time in a radial direction in the same way, as the total height of specimen, and formed the "rotor blades".

4. Discussion

4.1. Shape development and kinetics of oxidation

The significant increase of linear dimensions during the oxidation could not be explained only by the formation of oxide phases. The extensive swelling of new phases should accompany this process. This assumption was supported by microstructure observation and by the dependence of the final shape of the oxidized specimen on its initial geometry.

From the results of X-ray analysis it can be suggested that the oxidation of tungsten carbide could be described by the reactions [12].

$$WC + \tfrac{5}{2} O_2 \rightarrow WO_3 + CO_2, \text{ or} \quad (1)$$

$$WC + 2O_2 \rightarrow WO_3 + CO \quad (2)$$

These reactions assumed the formation of volatile gases besides WO_3. The comparison of the theoretically determined and experimentally measured weight gain proved this assumption: theoretical weight gain evaluated according to Equation 1 and/or Equation 2 only for the initial and final phases in the specimen yielded the value $(M_{WO_3} - M_{WC})/M_{WC} = 0.183$ (M_{WO_3} and M_{WC}, molecular weights of WO_3 and WC, respectively; atomic weight of W is $M_W = 183.8$, carbon $M_C = 12$ and oxygen, $M_O = 16$) which was in very good agreement with the weight gain of 18.5–19% determined experimentally. The small deviation can be connected with the presence of Co in studied materials that was not considered in the evaluation. The values of weight gain would be different for the reactions assuming the formation of other tungsten oxides (approximately 10% for WO_2 and 16% for W_4O_{11}).

The presence of volatile gas could explain the effect of swelling due to pore formation and their extensive growth. The gas pressure inside the pores at the temperature T can be estimated as follows: from one WC grain with size I and containing N molecules of WC ($N \approx I^3/\Omega_{WC}$, where Ω_{WC} = volume of one WC molecule) can arise the same amount – N molecules of WO_3 and N molecules of CO_2 or CO (see Equations 1 and 2). These molecules formed n moles of gas ($n = N/N_A$, N_A, Avogardro's number) and when they fill in the pore with size L, the gas pressure p inside this pore would be approximately $p = nRT/L^3 = nN_AkT/L^3 = (kT/\Omega_{WC})(I/L)^3$; ($R = N_Ak$; gas constant, $k = 1.3 \times 10^{-23}$ J mol^{-1}K, Boltzmann constant). The pressure inside the pore would be proportional to the cube of the ratio of linear dimensions of WC grains and pores. This pressure in the pores, which is comparable with the mean grain size ($I \approx L$), can reach at $T \approx 10^3$K and $\Omega_{WC} \approx 1 \times 10^{-29}$ m^3,

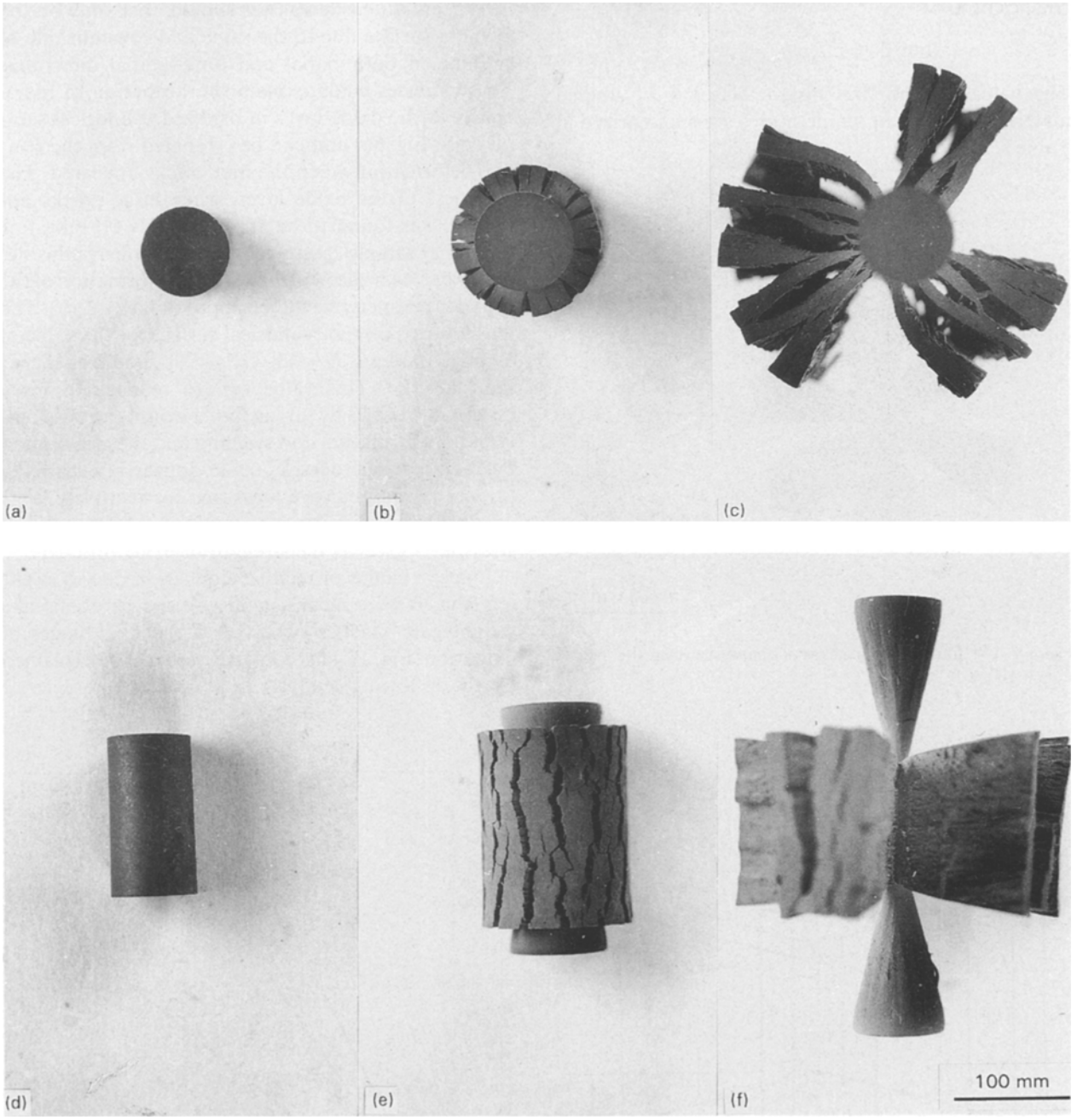

Figure 2 Shape change development of cylindrical sample (3 μm WC grain size, 6% Co) during oxidation at 700 °C (a–c, side view; d–f, top view): a,d, initial shape; b,e, after 80 min; c, f, after 510 min at 700 °C.

approximately $p \approx 1.4$ GPa. This is comparable with the rupture strength of WC–Co at studied temperatures (approximately 1.4–1.7 GPa at 600 °C and 1.0–1.3 GPa at 800 °C for similar grain size and cobalt content in vacuum [13–14] and considerably higher than the stress range in which creep deformation has been studied (83–220 MPa for 6 and 15% Co content at 750 and 650 °C, and up to 500 MPa at higher temperatures and in pure WC, respectively [15–16]). Such a high pressure inside the pores would be able to deform the ductile binder Co phase and cause their intensive swelling. On the initial stage of oxidation, when $L \ll I$, the pressure inside the pores should be even higher than the above calculated value. It can be expected that the swelling of the oxide layer would occur relatively fast on the oxidation front and develop up to the formation of open porosity.

The linear kinetics of oxidation can be seen to be directly due to the formation of regular cones and pyramids from the flat surfaces of cylindrical and cubic specimens, respectively. It would be possible only in the case of constant oxidation rate controlled by the reaction at the interface and constant swelling in all directions. The diffusion through the oxide layer could not be the rate-controlling process in this case, especially if the open porosity and sharp boundary between oxide and hard metal were observed. The tangent of the half angle at the top of the cone β should be proportional to the rate of initial radius of cylinder R_0 and the thickness of oxide layer after complete oxidation b (see Fig. 4) in this case. Assuming constant swelling after oxidation $b = \kappa R_0$, where κ is the swelling coefficient, the angle β should be proportional to the reciprocal value of swelling

coefficient κ

$$\tan \beta = R_0/b = 1/\kappa$$

The values of the swelling coefficient κ of studied materials at different temperatures are summarized in Table I.

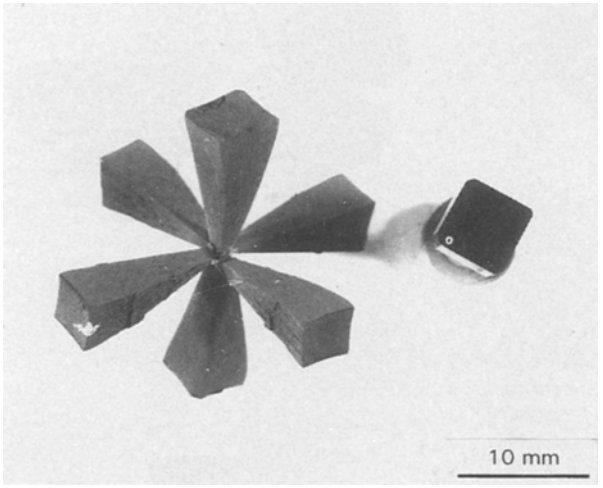

Figure 3 The initial and final shape of a cubic specimen after oxidation at 800 °C.

Tangential tensile stresses should arise only on the cylinder surface due to the same and constant rate of swelling in both radial and longitudinal directions. These stresses could explain the formation of radial cracks in the oxide layer in oxidized cylindrical samples (see Fig. 6b) and can be estimated from the relative deformation when the first cracks appeared. The thickness of the oxide layer, when large cracks appeared, was found to be approximately 0.1 mm. For the initial sample radius $R_0 = 3.5$ mm (the radius decrease can be neglected) the relative deformation of the cylinder perimeter would be approximately 2.8%. The tensile stress on the cylindrical surface for the value of Young's modulus $E \sim 450$ GPa [14], should be higher than 12 GPa. This value can be reduced to more reasonable values by taking into account the possibility of pore formation and swelling and the assumption that the first microcracks could appear in essentially thinner layers, than we measured for relatively large cracks. Despite this it can be expected that the reduced stress level exceeds the strength of oxide products.

Linear kinetics of relative elongation due to swelling (Fig. 4) were inconsistent with the parabolic-like weight gain kinetics observed in the final stages of oxidation (Fig. 1). This contradiction can be explained by the following analysis in which the presence of

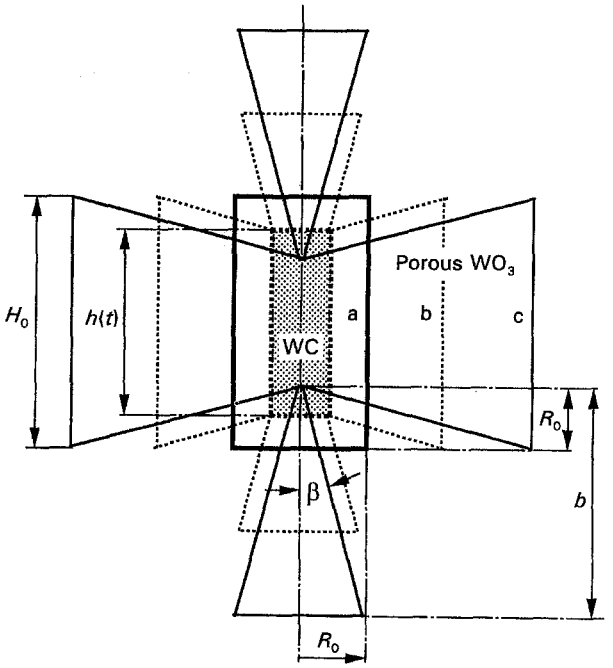

Figure 4 Scheme of the cross-sections of a cylindrical specimen at different stages of oxidation: a, initial; b, intermediate; c, final – after the complete oxidation (see Fig. 3a and c).

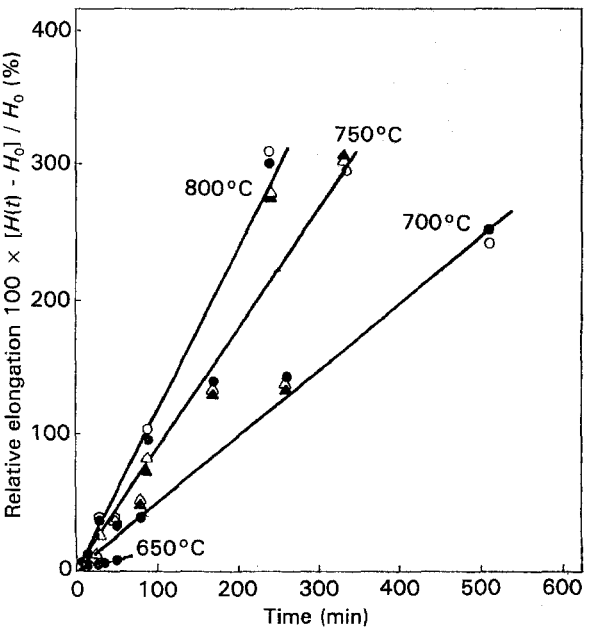

Figure 5 The kinetics of the relative elongation of WC–Co samples with different grain size and Co content during the oxidation. ○, 6% Co/3 μm WC; △, 6% Co/5 μm WC; ▲, 10% Co/5 μm WC; ●, 15% Co/3 μm WC.

TABLE I Top angles and swelling coefficients of WC–Co sintered carbides at different temperatures

Sample Co content (vol.%)/ mean grain size [μm]	Top angle 2β/swelling coefficient κ		
	Temperature 973 K (700 °C)	1023 K (750 °C)	1073 K (800 °C)
6/3	29°/3.86	24°/4.70	25°/4.51
6/5	32°/3.48	28°/4.01	24°/4.70
10/5	23°/4.91	22°/5.14	20°/5.67
15/3	28°/4.01	25°/4.51	21°/5.39

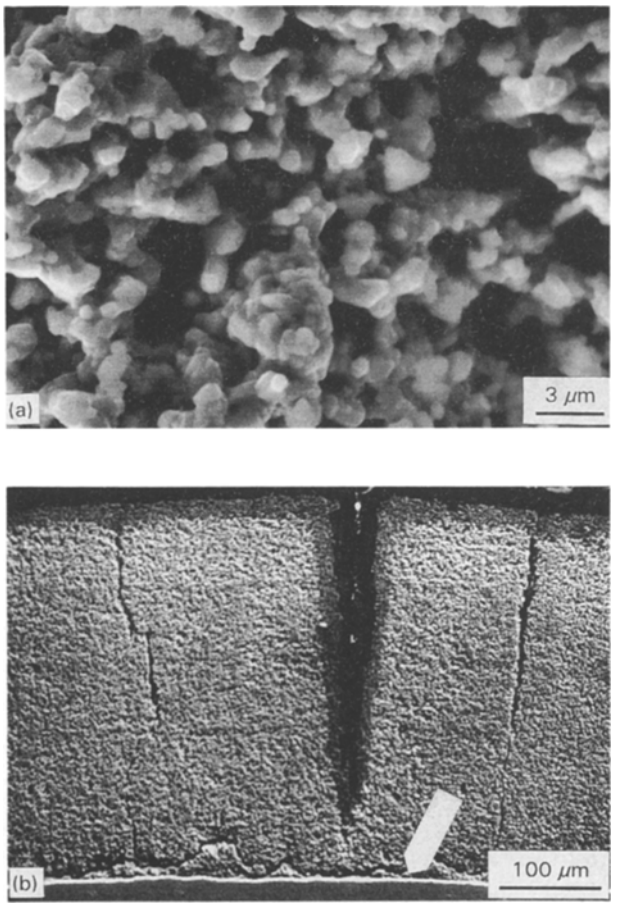

Figure 6 (a) Detail of the porous microstructure of the oxide layer; (b) sharp boundary between the oxide layer and WC–Co.

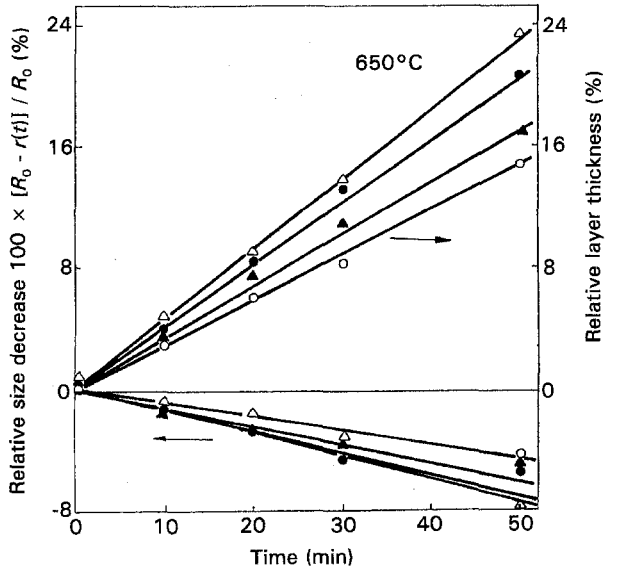

Figure 7 The kinetics of oxide layer thickness and diameter of unoxidized part of a cylindrical specimen measured on cross-section during oxidation at 650 °C. ○, 6% Co/3 μm WC; △, 6% Co/5 μm WC; ▲, 10% Co/5 μm WC; ●, 15% Co/3 μm WC.

the Co phase was neglected. The initial weight m_0 of the sample, which consists only of a large amount of WC grains, can be expressed through the total amount of WC molecules in the sample N_0 as $m_0 = M_{WC}(N_0/N_A)$. Because of the constant number of W atoms N_0 in the specimen, either in the form of WC or WO_3, the weight of the oxide phase, which arose from ΔN atoms of W, would be $M_{WO_3}(\Delta N/N_A)$, where ΔN is the reduction of N_0 due to the oxidation. The weight of the specimen $m(t)$, partially oxidized after time $t < t_{max}$, where t_{max} is the time to complete oxidation of the specimen, can be found as a sum of molecular weights of $N_0 - \Delta N$ molecules of WC and ΔN molecules of WO_3. The kinetics of relative weight change during oxidation can be described by the following equation

$$(m(t) - m_0)/m_0 = (M_{WO_3}/M_{WC} - 1)\Delta N/N_0$$

where $M_{WO_3}/M_{WC} = 1.183$. The ratio of the numbers of the oxidized and unoxidized WC molecules $\Delta N/N_0$ should be the same as the ratio of the volumes $\Delta V/V_0$,

$$\Delta N/N_0 = \Delta V/V_0$$

where V_0 is the initial volume of WC sample containing N_0 molecules and ΔV is the reduction of WC volume due to the oxidation of ΔN molecules of WC. Finally, the relative weight gain kinetics can be expressed as

$$(m(t) - m_0)/m_0 = (M_{WO_3}/M_{WC} - 1)\Delta V/V_0 \quad (3)$$

Equation 3 indicates that weight gain kinetics will be controlled by the relative volume decrease of the unoxidized part of the specimen $\Delta V/V_0 = (V_0 - V(t))/V_0$. It can be found from the assumption of constant rate of decrease of the radius $r(t)$ and height $h(t)$ of the WC part of cylindrical specimen

$$r(t) = R_0 - qt$$
$$h(t) = H_0 - 2qt, \quad (4)$$

where q is the rate of oxidation defined as $q = R_0/t_{max}$. The substitution of Equations 4 into Equation 3 gives the relative weight gain kinetics of the cylindrical specimen

$$(m(t) - m_0)/m_0 = (M_{WO_3}/M_{WC} - 1) \times [2(1 + R_0/H_0)\tau - (1 + 4R_0/H_0)\tau^2 + 2(R_0/H_0)\tau^3] \quad (5)$$

where dimensionless time τ was determined as $\tau = t/t_{max}$. The ratio R_0/H_0 is a geometric factor connected with the initial form of the specimen. The weight gain kinetics of cubic specimens was expressed in a similar way

$$(m(t) - m_0)/m_0 = (M_{WO_3}/M_{WC} - 1) \times (3\tau - 3\tau^2 + \tau^3) \quad (6)$$

The difference between Equations 5 and 6 is caused only by different specimen geometry.

Theoretical relative weight gain kinetics for a cylindrical specimen (Equation 5) was compared with the experimental results in Fig. 8. The relatively good agreement between the theoretical curve and experimental points confirmed that the kinetics of weight gain would be controlled by the linear decrease of WC part of specimen as it was concluded from the kinetics of dimensional changes. The deviations of experimental results and model curve at $\tau \approx 0.5$ and $\tau = 1$

can be connected with incomplete oxidation of WC grains in the intermediate stage of oxidation and with the contribution of Co at the final stage, respectively.

4.2. Apparent activation energy

The apparent activation energy Q_{app} of the studied process of oxidation and swelling can be evaluated from the Arrhenius plot of the oxidation rates at different temperatures. However, weight gain kinetics (see Equations 3, 5 and 6) is not suitable for the determination of the oxidation rates, because of its nonlinear dependence ($d[(m(t) - m_0)/m_0]/dt \approx d(\Delta V/V_0)/dt \approx q + Aq^2t + Bq^3t^2$; A, B are coefficients of proportionality). The true rate q can be determined from the slope of the weight kinetics curve only on the initial stage of oxidation, when it is almost linear (Aq^2t and Bq^3t^2 are small in comparison with q). The determination of oxidation rates q from the kinetics of the unoxidized part of the specimen decrease (Equation 4 and Fig. 7.) and measurement of t_{max} (and formula $q = R_0/t_{max}$) was preferred. The resulting rates q determined by both methods and the values of the apparent activation energies are summarized in Table II. The mean values of apparent activation energy Q_{app} were within the range 45–67 kJ mol^{-1}. Weight gain kinetics on the initial stage of oxidation gave very similar results (32–52 kJ mol^{-1}), as can be expected from above-mentioned analysis. These values are considerably lower than the apparent activation energy of creep deformation, $\approx$ 540 kJ mol^{-1}, reported for similar WC–Co materials at stresses up to 200 MPa [16]. We concluded that the measured values of apparent activation energy are connected mainly with the reaction at the interface despite possible plastic deformation of the binder phase and the rearrangement of oxide grains in it, indicated by intensive swelling.

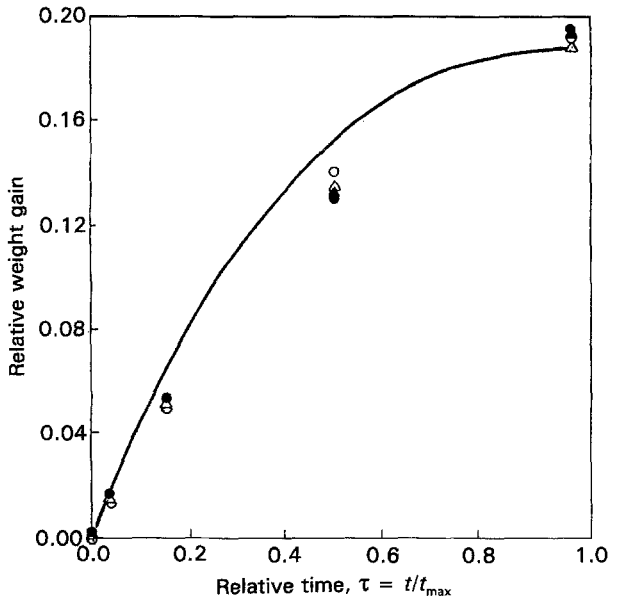

Figure 8 The comparison of experimentally measured and theoretically predicted relative weight gain kinetics of WC–Co oxidation at 700 °C. ○, 6% Co/3 μm WC; △, 6% Co/5 μm WC; ▲, 10% Co/5 μm WC; ●, 15% Co/3 μm WC.

4.3. The influence of microstructure characteristics

The examination of experimental data showed the minimum oxidation rates and swelling coefficients for materials with 6% Co. The dependence of these parameters on grain size of WC was not so clear because of small differences of grain size between the studied materials, but the tendency of the decrease of oxidation rate and swelling coefficient can be seen for those with larger grains.

Cobalt as a binder phase seemed to play an important role in the studied process. The numerous previous works on pure WC revealed only the formation of very brittle layers or complete loss of specimen shape after oxidation. The existence of a highly porous, but still rigid skeleton with a rotor- or cross-like form after oxidation would be possible due to the binding of oxide grains by Co. The occurrence of swelling would be also dependent on the presence of cobalt – the pressure of gas inside the pores could be relaxed due to the plastic deformation of Co or sliding of oxide grains in the binder phase. Consequently, smaller grain size and higher cobalt content should allow greater swelling, as observed experimentally (see Tables I and II).

4.4. The model of oxidation of WC–Co accompanied by swelling

The oxidation kinetics of studied materials can be limited either by diffusion or by reaction at the interface. It was shown in Section 4.2 that the reaction at the interface of WC grains should control the kinetics of oxidation. The WC grain oxidized directly in contact with oxygen (Fig. 9b) at the initial stage of oxidation and formed porous WO_3 grains. Cobalt covering the

TABLE II Oxidation rate of WC–Co sintered carbides at different temperatures

Temperature (K)	Oxidation rate q ($\times 10^{-8}$) (m s^{-1}) 6%Co/3 μm WC	6%Co/5 μm WC	10%Co/5μm WC	15%Co/3μm WC
923	5.0	1.4	7.5	9.0
973	7.7	7.5	7.6	7.7
1023	11.5	11.1	11.9	12.3
1073	14.4	12.6	19.6	16.5
Apparent activation energy Q_{app} ± standard deviation (kJ mol^{-1})				
	59.2 ± 4.0	44.9 ± 11.8	53.9 ± 14.8	66.9 ± 6.8

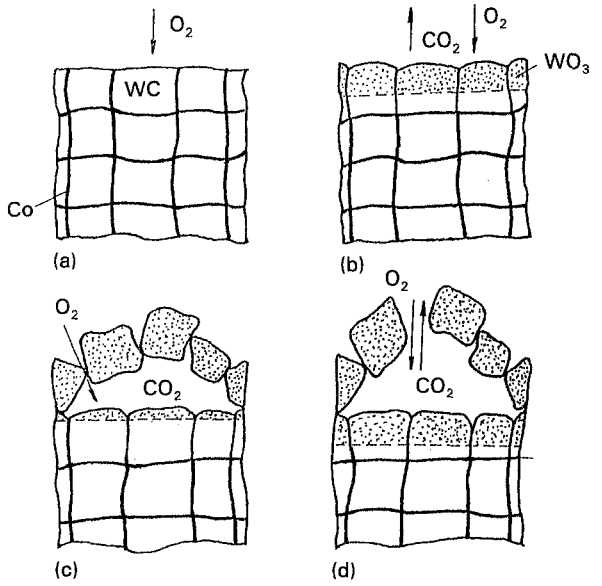

Figure 9. The schematic model of the oxidation of WC–Co alloys accompanied by swelling.

WC grains could limit both oxygen admission to WC and CO_2 exhaust after the reaction (Equation 1). However, because of fast oxygen diffusion through the thin cobalt phase, indicated by linear kinetics, volatile gas formation at the interface of the $WC(WO_3)/Co$ phase can cause the nucleation and rapid growth of cavities. The binder phase can deform, the oxide grains rearrange in it and cavities can grow until the formation of open porosity (see Fig. 9c). As a result, swelling can be observed on a macroscopic scale. This model could explain the observed linear kinetics, approximately constant swelling coefficient and influence of WC grain size and Co content on oxidation behaviour.

5. Conclusions

The oxidation of studied WC–Co alloys in the temperature range 650–800 °C was found to be accompanied by extensive swelling of the porous oxide layer (up to 350% of initial size) due to the development of WO_3 and volatile gas that filled the pores and caused their growth. The oxidation showed linear kinetics with apparent activation energy within the range of 44–67 kJ mol^{-1}. It was proposed that the kinetics of oxidation was controlled by reaction at the interface. The oxidation rates and swelling coefficients increased when the mean size of WC grains was decreased and cobalt content increased. A possible model of WC–Co alloys' oxidation and swelling was proposed for the observed shape development and kinetics of the oxidation.

Acknowledgement

The authors are very grateful to M. Černik for X-ray experiments and to G. Leitner for helpful discussion.

References

1. K. J. A. BROOKES, "World Directory and Handbook of Hardmetals" (Int. Carbide Data, 4th edition, 1987).
2. J. DUSZA, L'. PARILÁK, M. ŠLESÁR and J. DIBLÍÍK, *Ceram. Int.* **9** (1983) 2.
3. J. DUSZA, L' PARILÁK and M. ŠLESÁR, *Ceram. Int.* **13** (1987) 133.
4. N. TSUCHIYA, M. FUKUDA, T. NAKAI and H. SUZUKI, *J. Jap. Soc. Powder met.* **6** (1991) 505.
5. R. KIEFFER, and F. KOLBL, *Z. Anorg. Chem.* **262** (1950) 97.
6. G. V. SAMSONOV, "Tugoplavkije sojedinenija" (Metallurgizdat, Moskva, 1963).
7. R. F. VOJTOVICH and E. A. PUGACH, *Poroshkovaya Metallurgija* (1973) 59.
8. R. F. VOJTOVICH and E. A. PUGACH, "Okislenije tugoplavkich soedinenij" (Metallurgizdat, Moskva, 1978).
9. YU. F. KOTS, V. S. PANOV, N. V. SHIPKOV and A. A. FILIMONOVA, *Poroshkovaya Metallurgija* (1990) 62.
10. B. O. HAGLUND and B. LEHTINEN, in "Proceedings of 3rd International Conference on Thermal Analysis" ICTA, Davos, Vol. 3 (1971) p. 545.
11. S. SHIMADA and M. KOZEKI, *J. Mat. Sci.* **27** (1992) 1869.
12. R. F. VOJTOVICH "Okislenie karbidov i nitridov" (Naukova dumka, Kiev, 1981).
13. G. S. KREIMER, in "Strength of Hard Alloys" (Consultant Bureau, Plenum Press, New York, 1968) in B. Johannesson, "The Fracture Behavior of Hardmetals", PhD. Thesis (Chalmers University of Technology, Göteborg, 1987) p.7.
14. N. BOUAOAUDJA, G. ORANGE, G. FANTOZZI, F. THEVENOT and P. GOEURIOT, *J. de Physique* **47** (1986) C1–739.
15. E. A. ALMOND, in "Science of Hard Materials" edited by R. K. Wisandham, P. J. Rowcliffe and J. Gurland (Plenum Press, New York, 1983) p. 517.
16. S. LAY, F. OSTERSTOCK, "Deformation of Ceramic Materials II.", *Mat. Sci. Res.* **18** (Plenum Press, New York, 1984) p. 463.

Received 23 September 1993
accepted 28 June 1994